Current rectification by simple molecular quantum dots: An *ab initio* study

B. Larade and A. M. Bratkovsky
Hewlett-Packard Laboratories, 1501 Page Mill Road, Palo Alto, California 94304, USA
(Received 12 April 2003; revised manuscript received 15 July 2003; published 5 December 2003)

We calculate current rectification by molecules containing a conjugated molecular group sandwiched between two saturated (insulating) molecular groups of different lengths (molecular quantum dot) using an *ab initio* nonequilibrium Green's function method. In particular, we study $S(CH_2)_m—C_{10}H_6—(CH_2)_nS$ with naphthalene as the conjugated central group. The rectification current ratio ~ 35 has been observed at $m=2$ and $n=10$, due to resonant tunneling through the molecular orbital (MO) closest to the electrode Fermi level (lowest unoccupied MO in the present case). The rectification is limited by the interference of other conducting orbitals, but can be improved by, e.g., adding an electron withdrawing group to the naphthalene.

DOI: 10.1103/PhysRevB.68.235305 PACS number(s): 85.65.+h

I. INTRODUCTION

An effective current rectifier is a necessary element of electronics circuitry. Aviram and Ratner suggested in 1974 that in a molecule containing donor (*D*) and acceptor (*A*) groups separated by a saturated σ-bridge (insulator) group, the (inelastic) electron transfer will be more favorable from *A* to *D*, rather than in the opposite direction.[1] It was noted more recently that the electron transfer from *D* to *A* should start at smaller bias voltage because the highest occupied molecular orbital (HOMO) is centered on the *D* group, whereas the lowest unoccupied molecular orbital (LUMO) is located on the acceptor group *A*. The onset of resonant tunneling in this case corresponds to the alignment of the HOMO on the *D* group with the LUMO on the *A* group under external bias voltage, which are closest in energy.[2] The molecular rectifiers synthesized in the laboratory were of somewhat different *D*-π-*A* type, i.e., the ''bridge'' group was conjugated.[3,4] The molecule $C_{16}H_{33}—\gamma$Q3CNQ can be viewed as fused naphthalene and tetracyanoquinodimethane molecules with an attached $C_{16}H_{32}$ alkane ''tail,'' needed to provide enough van der Waals attraction between the molecules to assemble them into a Langmuir-Blodgett film on a water surface. Although the molecule did show rectification (with considerable hysteresis), it performed not like a conductor but rather like an anisotropic insulator because of the large alkane tail. Indeed, the currents reported in Ref. 4 were of the order of 10^{-17} A/molecule, which make its application impractical. It was recently realized that in this molecule the resonance does not come from the alignment of the HOMO and LUMO, since they cannot be decoupled through the conjugated π bridge, but rather due to an asymmetric voltage drop across the molecule where the HOMO and LUMO are asymmetrically positioned with respect to the Fermi level of the electrodes.[5] It is not clear if this mechanism has been observed. For instance, the contact between the alkane chain and electrode was certainly poor, via weak van der Waals forces. No temperature dependence of the resistivity was reported, but its large value suggests that inelastic tunneling processes may have been involved.

It is clear that the rectifying molecular films built with the use of the Langmuir-Blodgett technique, relying on long aliphatic (or other insulating) tails, will produce hugely resistive molecules not suitable for moletronics applications. There are reports of rectifying behavior in other classes of molecules, e.g., molecules chemisorbed on electrodes, where an observed asymmetry of the *I*-*V* curves is likely due to asymmetric contact with the electrodes,[6,7] or an asymmetry of the molecule itself.[8]

To achieve good rectification by a molecule with a reasonable conductivity, one should avoid using molecules with long saturated (insulating) groups, which would make them prohibitively resistive. Thus, a suggestion to use relatively short molecules with certain end groups to allow their self-assembly on a metallic electrode's surface seems to be very attractive.[9] In that previous paper the transport through a phenyl ring connected to electrodes by asymmetric alkane chains $(CH_2)_n$ has been calculated with the use of a semiempirical tight-binding method. Since the microscopic parameters of the model are poorly known, especially hopping integrals between the molecule and electrodes, the electrode work function, and the affinity of the molecule (which may be strongly affected by bonding to a metal), the calculations have been performed for a number of these parameters. The calculations indicated a rectification ratio for the $—S—(CH_2)_2—C_6H_4—(CH_2)_n—S—$ molecule of about 100 for $n=10$, with a resistance $R \approx 13$ GΩ. It is difficult to know how quantitative these numbers are, because of a limited basis set and uncertainty in the parameters of the model. For instance, accounting for a larger basis set for wave functions may lead to an increased estimate of the tunnel current, since the system may have more channels to conduct current.

The idea[9] of a molecular rectifier with one conjugated ring has been tried in a recent work.[10] The molecules in this study consisted of a phenyl or thiophene ring attached to a $(CH_2)_{15}$ tail by a CO group. The molecules have been self-assembled on a Si surface functionalized in the usual manner by SiO_2. Rectification behavior has been clearly observed with a maximum value of about 37, with most samples having the rectification ratio $\lesssim 10$. One may note that the insulating tail was rather long, so that inelastic tunneling processes may have been present. In this respect, measurements at different temperatures may shed some light on the nature of transport in these samples.

Experimentally, it may be easier to synthesize somewhat different compounds with a naphthalene group as a

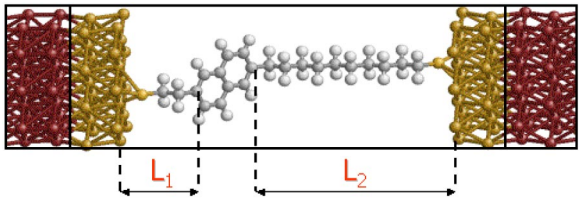

FIG. 1. (Color online) Schematic diagram of typical Au-molecular rectifier-Au device structure analyzed within our *ab initio* formalism. Electrodes are represented as (3×3) Au(111) surfaces, with the terminal sulfurs of the molecule positioned 1.8 Å above the triangular hollow site of the electrodes (Ref. 16). The L_1 (L_2) indicates the insulating barrier length separating the molecular conducting unit from the left (right) electrode.

"molecular quantum dot," such as —S—$(CH_2)_m$—$C_{10}H_6$—$(CH_2)_n$—S—,[11] which we will also refer to as —S—$(CH_2)_m$—Naph—$(CH_2)_n$—S—. To obtain an accurate description of transport in this case, we employ an *ab initio* nonequilibrium Green's function method.[12]

The calculation shows that indeed the current rectification $I_+/I_-\sim100$ may be possible for some designs such as —S—$(CH_2)_2$—Naph—$(CH_2)_{10}$—S—, where $I_{+(-)}$ is the forward (reverse) current. The difference between the forward and reverse voltages is, however, limited by other orbitals intervening into the conduction process. One needs the conducting orbital to be much closer in energy to the electrode Fermi level than the other ones (e.g., LUMO versus HOMO) and this energy asymmetry can be manipulated by "doping" the conjugated conducting part by attaching a donor (or acceptor) group, as will be shown below.

The present calculation takes into account only elastic tunneling processes. Inelastic processes may substantially modify the results in the case of strong interaction of the electrons with molecular vibrations, see Ref. 13. If the inelastic processes are important, one should observe steps in the *I-V* curve at energy intervals corresponding to the energies of the excited vibrons, at least at low temperatures,[13] as observed in Ref. 14. It would be interesting, therefore, to perform current measurements on the family of present rectifiers at low temperatures. There are indications in the literature that the carrier might be trapped in a polaron state in saturated molecules somewhat longer than those we consider in the present paper.[15] The present design should avoid these effects, since we deliberately choose relatively shorter barrier groups. This alleviates a possibility of trapping the charges on the conjugated group, since the left barrier is selected to be relatively transparent, in order that the transport not be affected by Coulomb blockade effects (see details in the following section).

II. RECTIFICATION BY MOLECULAR QUANTUM DOT

The structure of the present molecular rectifier is shown in Fig. 1. The molecule consists of a central conjugated part (naphthalene) isolated from the electrodes by two insulating "arms" built from saturated aliphatic chains $(CH_2)_n$ with lengths L_1 (L_2) for the left (right) chain. The principle of

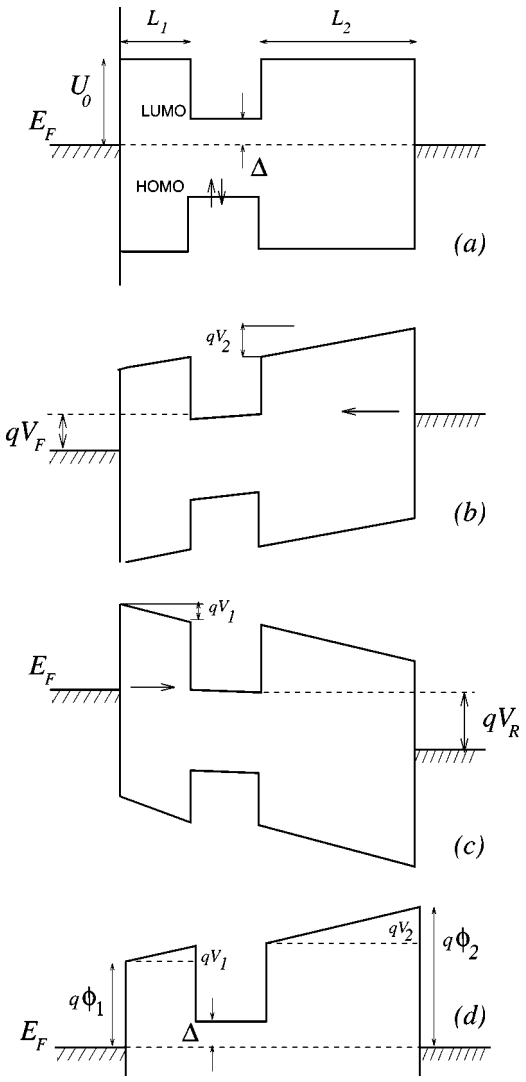

FIG. 2. Schematic band diagram of the molecular rectifier. The middle narrow-band part represents the naphthalene conjugated group. The barrier height $U_0=4.9$ eV (present theory), 4.8 eV (experiment Ref. 13). Panels (a)–(c): unbiased, forward, and reverse biased rectifier with similar electrodes. Panel (d): unbiased rectifier with dissimilar electrodes. At equilibrium, there is a voltage drop $qV_{1(2)}$ across the left (right) barrier.

molecular rectification by a molecular quantum dot is illustrated in Fig. 2, where the electrically "active" molecular orbital, localized on the middle conjugated part, is the LUMO, which lies at an energy Δ above the electrode Fermi level at zero bias. The position of the LUMO, for instance, is determined by the work function of the metal $q\phi$ and the affinity of the molecule $q\chi$, $\Delta=\Delta_{\mathrm{LUMO}}=q(\phi-\chi)$. The position of the HOMO is given by $\Delta_{\mathrm{HOMO}}=\Delta_{\mathrm{LUMO}}-E_g$, where E_g is the HOMO−LUMO gap. If this orbital is considerably closer to the electrode Fermi level E_F, then it will be brought into resonance with E_F prior to other orbitals when the molecule is biased in either the forward or the reverse direction (Fig. 2). It is easy to estimate the forward and reverse bias voltages, assuming that the voltage mainly falls off at the saturated (wide band gap) parts of the molecule with the lengths L_1 (L_2) for the left (right) barrier, Fig.

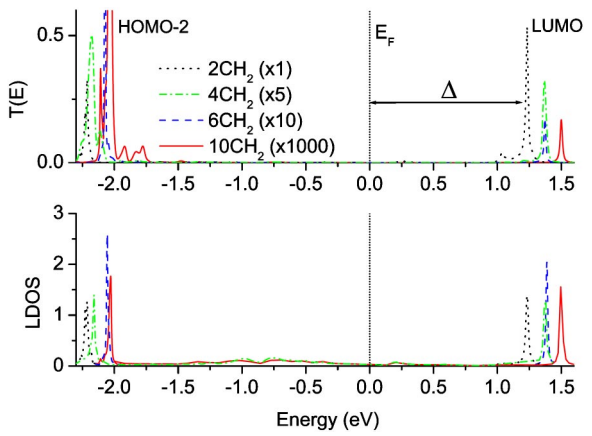

FIG. 3. (Color online) Transmission coefficient (top) and local density of states (bottom) vs energy E for rectifiers —S—$(CH_2)_2$—$C_{10}H_6$—$(CH_2)_n$—S—, $n=2,4,6,10$. Δ indicates the distance of the closest MO to the electrode Fermi energy ($E_F=0$).

2. Since the voltage drops proportionally to the lengths of the barriers, $V_{1(2)} \propto L_{1(2)}$, we obtain for the partial voltage drops $V_{1(2)}=VL_{1(2)}/L$, where V is the bias voltage. Forward and reverse voltages are then found from the resonance condition, which gives

$$V_F=\frac{\Delta}{q}(1+\xi), \tag{1}$$

$$V_R=\frac{\Delta}{q}\left(1+\frac{1}{\xi}\right), \tag{2}$$

$$V_F/V_R=\xi\equiv L_1/L_2, \tag{3}$$

where q is the elementary charge. A significant difference between forward and reverse currents should be observed in the voltage range $V_F<|V|<V_R$. For our systems in question the parameter $\Delta=1.2$–1.5 eV, Fig. 3, the value being determined by the work function of the electrodes and the electron affinity of the conjugated part of the molecule, as well as by the strength of a surface dipole layer. For unlike electrodes with the work functions $q\phi_1$ and $q\phi_2$ there will be a built-in potential in the system $q\phi_b=q(\phi_2-\phi_1)$, Fig. 2(d). In this case the expressions for the forward and reverse bias voltages are modified as follows:

$$V_F=\left(\frac{\Delta}{q}+\phi_b\right)(1+\xi), \tag{4}$$

$$V_R=\phi_b+\frac{\Delta}{q}\left(1+\frac{1}{\xi}\right). \tag{5}$$

Thus, the operating bias "window" in this case is

$$V_R-V_F=(V_R-V_F)_0-\xi\phi_b=\frac{\Delta}{q}\left(\frac{1}{\xi}-\xi\right)-\xi\phi_b. \tag{6}$$

Therefore, it slightly ($\xi<1$) *increases* when $\phi_b<0$ ($\phi_1>\phi_2$, left work function is larger), and *shrinks down* when $\phi_b>0$ (right work function is larger). One would like to use as asymmetric a molecule as possible to increase the operating voltage, and in this case the difference of the work functions of the electrodes progressively becomes less important.

The main transport features of the present system can be qualitatively explained within a model of resonant tunneling through a localized state (molecular orbital) in the barrier. The current can be written as

$$I=\frac{2q}{h}\int dET(E)[f(E)-f(E+qV)], \tag{7}$$

where the transmission $T(E)$ at zero temperature is given by (for two spin directions)

$$T(E)=\frac{\Gamma_L\Gamma_R}{(E-E_{MO})^2+(\Gamma_L+\Gamma_R)^2/4}, \tag{8}$$

where $E_{MO}=\Delta-qV_1=\Delta-qVL_1/L$ is the energy of the molecular orbital, relative to the Fermi level of the left electrode. The transmission is maximal and equals unity when $E=E_{MO}$ and $\Gamma_L=\Gamma_R$, which corresponds to a symmetric position of the central conjugated part with respect to the electrodes. We can estimate $\Gamma_{L(R)}\sim t^2/D=\Gamma_0 e^{-2\kappa L_{1(2)}}$, where t is the overlap integral between the molecular orbital (MO) and the electrode, D is the electron bandwidth in the electrodes, and κ the inverse decay length of the resonant MO into the barrier. The latter quantity can be estimated from $\hbar^2\kappa^2/2m^*=U_0$, where U_0 is the barrier height [$\approx$4.8 eV in alkane chains $(CH_2)_n$,[15] $\approx$5 eV from density-functional theory (DFT) calculations] and $m^*\lesssim 1$ the effective tunneling mass. The current above the threshold (when the resonant tunneling condition is met) is given by

$$I\approx\frac{2q}{\hbar}\Gamma_0 e^{-2\kappa L_2}. \tag{9}$$

We see immediately that increasing the spatial asymmetry of the design (i.e., increasing L_2/L_1) changes the operating voltage range linearly, $V_R-V_F\approx(\Delta/q)L_2/L_1$, and brings about an *exponential* decrease in current.[9] This severely limits the ability to increase the rectification ratio while simultaneously keeping the resistance of the molecule at a reasonable value. One therefore needs a quantitative analysis of all microscopic details, including the molecule-electrode contact, and the potential and charge distribution, in order to make comparisons with the data.

III. METHOD

Since we study relatively shorter molecules, electron transport is likely to proceed elastically. We shall treat the elastic tunneling processes from first principles in order to evaluate all the relevant microscopic characteristics within the density-functional theory. This allows us to check the accuracy of the semiempirical methods used previously, and find results for new objects of experimental interest, such as the present molecular quantum dot with a naphthalene conjugated middle group. We use an *ab initio* approach that combines the Keldysh nonequilibrium Green's function (NEGF) (Ref. 18) with pseudopotential-based real space

DFT.[12] In contrast to standard DFT work, our NEGF-DFT approach considers a quantum-mechanical system with an *open* boundary condition provided by semi-infinite electrodes under external bias voltage. The main advantages of our approach are (i) a proper treatment of the open boundary condition; (ii) a fully atomistic treatment of the electrodes, and (iii) a self-consistent calculation of the nonequilibrium charge density using NEGF. Details of the method have been presented elsewhere,[12] and here we briefly outline the main points.

For the open devices studied here, our system can be divided into three regions, a left and a right electrode and a central scattering region, which contains a portion of semi-infinite electrodes (see Fig. 1). This division effectively reduces the infinitely large problem to one defined inside a finite scattering region, by using the fact that deep inside our electrodes, the effective Kohn-Sham (KS) potential $V^{eff}[\rho(r)]$ corresponds to the bulk KS potential. Boundary conditions on the central scattering region, which corresponds to our DFT simulation cell, can then be written,[12]

$$V^{eff}=\begin{cases} V_l^{eff}(r)=V_{l,\mathrm{bulk}}(r), & z<z_l \\ V_c^{eff}(r), & z_l<z<z_r \\ V_r^{eff}(r)=V_{r,\mathrm{bulk}}(r), & z>z_r, \end{cases} \tag{10}$$

where the planes $z_{l(r)}$ are the left (right) scattering region boundaries. External bias voltage is then applied as a boundary condition for the Poisson equation in our central scattering region, which is self-consistently solved on a three-dimensional (3D) real space grid using a multigrid approach. By including atomic layers of the electrode in our scattering region, we provide a proper treatment of the electrode-molecule interaction, and allow for the effective screening of the molecule away from our molecular junction. Importantly, our atomic electrodes are computed within the same model chemistry, using a standard self-consistent DFT approach. The contributions of our semi-infinite electrodes to the scattering region are then incorporated explicitly through the self-energies in the Green's function. Furthermore, the additional layers of atomic electrode included into the scattering region allows us to consider the effects of charge transfer, and implicitly accounts for the alignment of molecular orbitals to the electrode Fermi energy [for the Au(111) electrodes considered here, the work function was found to be $\sim$5.3 eV]. Finally, the nonequilibrium density matrix $\hat{\rho}$ is constructed via NEGF,[18]

$$\hat{\rho}=\frac{1}{2\pi i}\int dE\,\mathrm{Tr}G^{<}(E), \tag{11}$$

where the lesser Green's function is determined from the operator relation

$$G^{<}=G^{R}\Sigma^{<}G^{A}, \tag{12}$$

via the retarded (advanced) Green's functions $G^{R(A)}$, and $\Sigma^{<}$ corresponds to the self-energy part describing an injection of charge into the scattering region (molecule) from the electrodes. This process is characterized by the usual *open channel* representation of the scattering states with momenta k_l^n (k_r^n) in the left (right) electrodes, where index n enumerates all open channels (available Bloch states of the electrons in the electrodes). The Fermi functions $f(k_l^n)$ and $f(k_r^n)$ define the occupied states in the leads to be accounted for in an evaluation of the electron transport. To evaluate the Green's function, one treats the *disconnected* system consisting of the left (right) lead marked by index $l(r)$ and the scatterer c. The transport Green's function is then found from the Dyson equation

$$(G^R)^{-1}=(G_0^R)^{-1}-V, \tag{13}$$

where the unperturbed retarded Green's function is defined in operator form as

$$(G_0^R)^{-1}=(E+i0)\hat{S}-\hat{H},\quad \hat{H}=\begin{pmatrix} H_{l,l} & H_{l,c} & 0 \\ H_{c,l} & H_{c,c} & H_{c,r} \\ 0 & H_{r,c} & H_{r,r} \end{pmatrix}. \tag{14}$$

H is the Hamiltonian matrix, $H_{c,l}=H_{l,c}^{\dagger}$, $H_{r,c}=H_{c,r}^{\dagger}$, S is the *overlap* matrix, $S_{i,j}=\langle\chi_i|\chi_j\rangle$, for nonorthogonal basis set orbitals χ_i, and the coupling of the scatterer to the leads is given by the Hamiltonian matrix $V=\mathrm{diag}[\Sigma_{l,l},\,0,\,\Sigma_{r,r}]$. In all formulas above, it is assumed that the matrix elements are given in terms of the nonorthogonal basis set.

The self-energy part $\Sigma^{<}$, which is used to construct the nonequilibrium electron density in the scattering region, is found from

$$\Sigma^{<}=-2i\mathrm{Im}[f(E)\Sigma_{l,l}+f(E+qV)\Sigma_{r,r}], \tag{15}$$

where $\Sigma_{l,l(r,r)}$ is the self-energy of the left (right) electrode, calculated for the semi-infinite leads using an iterative technique.[12,19] $\Sigma^{<}$ accounts for the steady charge ''flowing in'' from the electrodes. The transmission probability is given by

$$T(E)=4\mathrm{Tr}[\mathrm{Im}(\Sigma_{l,l})G_{l,r}^{R}\mathrm{Im}(\Sigma_{r,r})G_{r,l}^{A}], \tag{16}$$

from which we obtain the current as

$$I=\frac{2e}{h}\int_{\mu_R}^{\mu_L}dE[f(E)-f(E+qV)]T(E,V), \tag{17}$$

where $\mu_L-\mu_R=qV$. The local density of states, which is a very important quantity to characterize the spatial character of the wave functions, can be obtained from

$$N(E,\vec{r})=\frac{1}{2\pi i}\mathrm{Tr}[G^{<}(E)|\chi(\vec{r})\rangle\langle\chi(\vec{r})|]. \tag{18}$$

To construct the system Hamiltonian, we use self-consistent DFT within the local-density approximation. The atomic cores are defined using standard norm-conserving nonlocal pseudopotentials,[20] and we expand the Kohn-Sham wave functions in a fireball[21] *s*-, *p*-, *d*- real-space atomic orbital basis.[12,22] The Green's function is determined by direct matrix inversion. External bias is incorporated into the Hartree potential, and in this way the nonequilibrium charge density

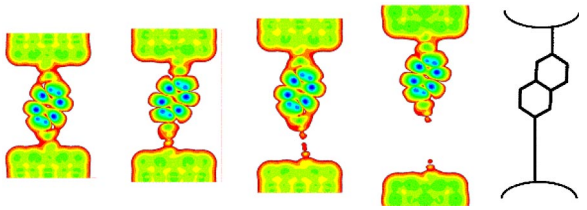

FIG. 4. (Color online) Local density of states $N(E_{\mathrm{LUMO}},\vec{r})$, projected onto a 2D grid defined by the plane of our central molecule, for the naphthalene series, $n=2,4,6,10$ from left to right, respectively. As the alkane chain increases in length, the coupling of the naphthalene group to the bottom electrode decreases. The stick figure on the far right illustrates the junction orientation.

is iterated to self-consistency, after which the current-voltage (I-V) characteristics have been computed.

IV. RESULTS

The physical picture of the transmission through a series of rectifiers —S—$(CH_2)_m$—$C_{10}H_6$—$(CH_2)_n$—S— for $m=2$ and $n=2,4,6,10$ is illustrated in Figs. 3 and 4. The transmission coefficient $T(E)$ (top panel) and the density of states $N(E)=\int dV N(E,\vec{r})$ (bottom panel) are shown at zero bias voltage in Fig. 3, with the electrode Fermi level taken as the energy origin. It follows from this figure that indeed the LUMO (Ref. 23) is the closest molecular orbital transparent to electron transport, and it is higher in energy than E_F by an amount $\Delta=1.2$–1.5 eV, depending on the molecule. Since the molecule is asymmetric, even at the resonance energy we have $T(E_{\mathrm{LUMO}})\lesssim 0.5$, Fig. 3. This can be traced back to the Breit-Wigner formula (8), which for $\Gamma_R \ll \Gamma_L$ gives $T(E_{\mathrm{LUMO}})\approx 4\Gamma_R/\Gamma_L < 1$, and it falls off as the asymmetry increases. There, the transmission through the HOMO and HOMO-1 states is negligible (these states are localized on the terminating sulfur atoms), but the HOMO-2 state conducts very well. As we shall see below, the HOMO-2 defines the threshold reverse voltage V_R, thus limiting the operating voltage range, Eq. (6).

The maps of the densities of states $N(E_{\mathrm{LUMO}},\vec{r})$ in Fig. 4 show the development of the tunneling gap between the naphthalene group and more distant electrode separated by an alkane chain $(CH_2)_n$, $n=2$–10. The symmetry and weight distribution of the LUMO in the device is very similar to the LUMO in the isolated molecule, telling us that the character of the molecular wave functions is preserved to a high degree. Obviously, in contact with electrodes molecular orbitals acquire some finite width $\Gamma=\Gamma_L+\Gamma_R$, and for highly asymmetric molecules $\Gamma\approx\Gamma_L$, so it is mainly defined by the transparency of the shorter (left) insulating group $(CH_2)_m$. One needs a rather small width Γ, which defines the sharpness of the voltage threshold for the current turn on.[9] We have calculated the molecules with $m=0,1,2$ with the results for $\Gamma_m=130$, 60, and 12 meV (Fig. 5). The last value for the left insulating group $(CH_2)_2$ seems to be most reasonable, since the resonant peak is rather narrow yet the molecule remains conductive. However, in some cases the short insulating group $(CH_2)_3$ may be preferential. This conclusion is similar to the one reached on the basis of the tight-binding model, but the peak positions and sizes are substantially different in both cases, the peak size being much larger in the case of the present DFT calculations, Fig. 5.

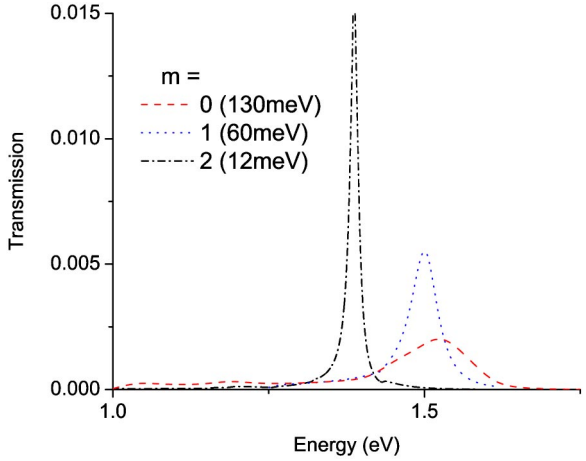

FIG. 5. (Color online) Transmission through molecular rectifiers —S—$(CH_2)_m$—$C_{10}H_6$—$(CH_2)_6$—S—, $m=0,1,2$. The peak corresponds to transmission through the LUMO state localized on the naphthalene ring. The numbers in parentheses indicate the peak width $\Gamma=\Gamma_L+\Gamma_R$ in meV.

Note that the molecule in the present design remains conductive, so that Coulomb blockade effects should not affect the transport. Indeed, the left barrier remains relatively transparent, with a substantial transmission probability through the LUMO, $T\approx 0.2$ for $m=2$, Fig. 3. The fact that the electron placed on the LUMO would quickly escape to the nearest electrode is obvious also from the map of the projected density of states at $E=E_{\mathrm{LUMO}}$, Fig. 4.

Our assumption that the voltage drop is proportional to the lengths of the alkane groups on both sides is quantified by the calculated potential ramp in Fig. 6. The plot is pro-

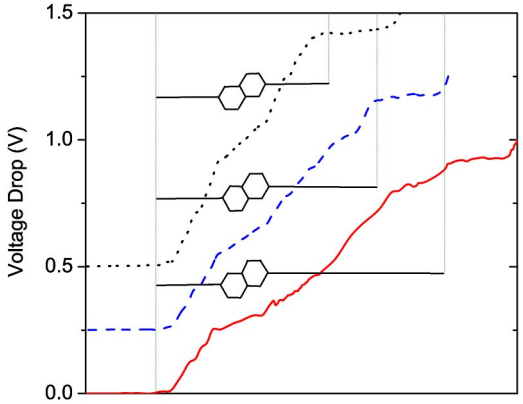

FIG. 6. (Color online) Potential drop as a function of position along the length (transport direction) of our molecular device, for the $n=2,6,10$ molecular rectifiers, at an applied bias voltage of 1 V. The drop is obtained by averaging the potential over a number of representative slices in the transverse direction. The positions of the naphthalene ring inside the junction are indicated by the stick figures, and the respective insulating barrier lengths are shown as horizontal lines. Curves are vertically shifted for clarity.

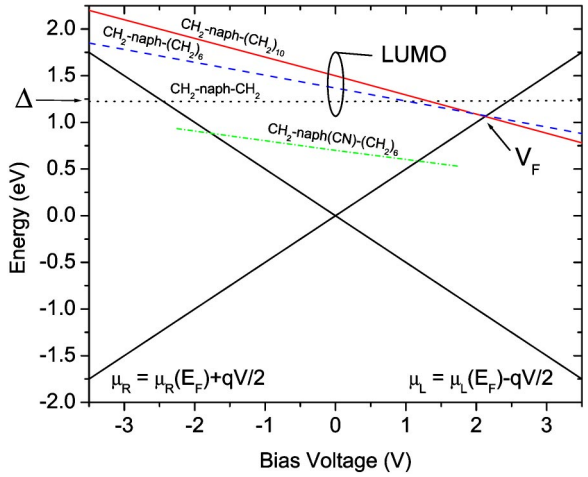

FIG. 7. (Color online) Evolution of the rectifier LUMO energy state as a function of applied bias voltage. Solid black lines represent the electrode chemical potentials, which are symmetrically shifted by the applied voltage $\mu_{R(L)}=E_F+(-)qV/2$. The forward voltage threshold corresponds to the crossing of the LUMO energy state with the right electrode chemical potential. In the case of a CN-doped naphthalene ring both the forward and reverse threshold voltages correspond to the LUMO crossing the electrode Fermi level, as in the ideal case, Fig. 2. In other systems, the HOMO-2 defines the reverse voltage threshold, thus reducing the operating voltage range.

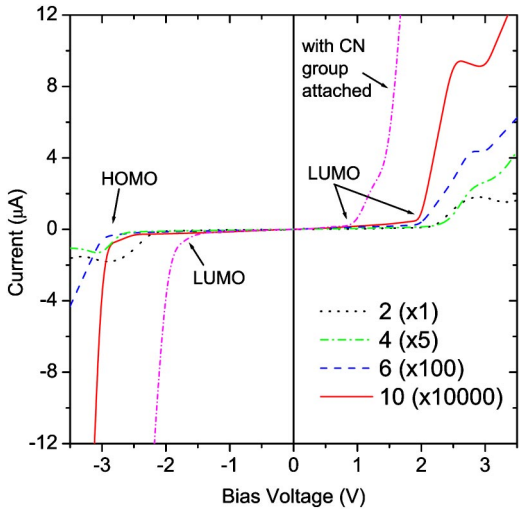

FIG. 8. (Color online) *I-V* curves for naphthalene rectifiers —S—$(CH_2)_2$—$C_{10}H_6$—$(CH_2)_n$—S—, $n=2,4,6,10$. The short-dash-dot curve corresponds to a cyano-doped (added group —C≡N) $n=10$ rectifier.

duced by averaging the full Hartree potential over a few representative slices (~20) in the transverse direction, with a grid spacing of $0.3a_0$ between them in the direction of current (where a_0 is the Bohr radius). The profile is close to a linear slope along the $(CH_2)_n$ chains. There is also a smaller but still noticeable voltage drop across the naphthalene group, which can be viewed as a fragment of wide-band semiconductor.

The threshold bias voltages can be obtained from Fig. 7, showing the evolution of the LUMO versus bias voltage with respect to the chemical potentials of the right (left) electrodes $\mu_{R(L)}=E_F+(-)qV/2$. The forward voltage corresponds to the crossing of the LUMO(V) and $\mu_R(V)$, which happens at about 2 V. An extrapolated crossing of the LUMO and μ_L occurs at large negative voltages but, unfortunately, this large desirable difference between V_F and V_R does not materialize. Although the LUMO defines the forward threshold voltages in all molecules studied here, the reverse voltage is defined by the HOMO-2 for "right" barriers $(CH_2)_n$ with $n=6,10$. The I-V curves are plotted in Fig. 8 and the corresponding parameters are listed in Table I. We see that the rectification ratio for current in the operation window I_+/I_- reaches a maximum value of 35 for the "2-10" molecule ($m=2$, $n=10$). It was estimated to be about 100 for the "2-10" molecule with a phenyl ring as a conjugated central part.[9] We have checked a series of molecules with a central phenyl ring and, unfortunately, do not find any significant rectification in this case, because the Fermi level in DFT calculations appears to lie close to mid gap. Thus, the tight-binding results for large rectification in one-phenyl ring molecules might have been a consequence of the model. Furthermore, the estimated resistance of the molecule in DFT is substantially less (2.8 GΩ) compared to the tight-binding model with a phenyl ring as a conjugated central unit (13 GΩ), see Table I.

One can manipulate the system in order to increase the energy asymmetry of the conducting orbitals (reduce Δ). To shift the LUMO towards E_F, one needs in effect to gate the naphthalene group by positive voltage. A chemical way of doing this would be to attach some chemical group, such as $-C\equiv N$ in the present case. The conjugated part would become 1-naphthalenecarbonitrile. If this molecule indeed remains stable with an addition of two aliphatic barrier groups, then one may observe an effect of such a chemical "doping" of the conjugated part. The $-C\equiv N$ group withdraws a fraction of an electron and acquires the negative charge $-\delta=-0.11q$. The charge is donated mainly by the naphthalene group, which acquires a positive charge and orbitals on the molecule shift to lower energies almost rigidly by about 0.6 eV, Fig. 9. The value of the shift is compatible with the value of the Hubbard electron-electron repulsion energy $U\approx 9$ eV on C atoms.[9] On the resulting *I-V* curve, both thresholds

TABLE I. The parameters for a set of the naphthalene-based rectifiers with various right insulating groups $(CH_2)_n$, Fig. 1. I_+/I_- the current rectification ratio, R the molecule resistance at bias voltage $V=2.5$ V.

n	Δ (eV)	V_F (V)	V_R (V)	V_{op} (V)	I_+/I_-	R (MΩ)
2	1.23	2.45	2.45		1	2.20
4	1.37	2.50	3.00	2.50	5	20.1
6	1.39	2.15	3.13	2.50	15	90.9
6 [a]	0.71	1.05	1.85	1.75	25	11.03 [b]
10	1.50	2.10	2.85	2.50	35	2780
10 [a]	0.81	1.18	2.50	1.75	85	1287 [b]

[a]CN doped.

[b]Resistance at $V=1.75$ V.

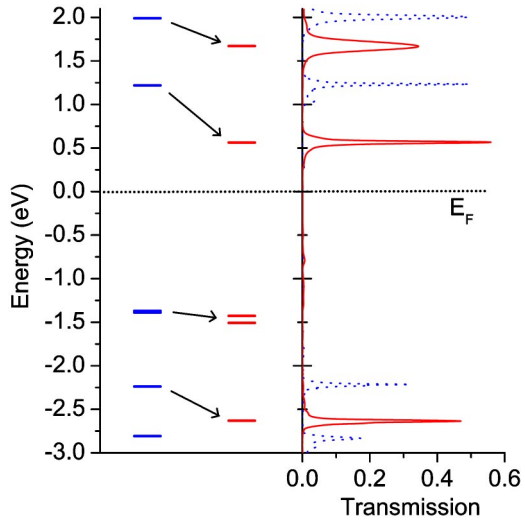

FIG. 9. (Color online) Left: Energy-level positions for undoped and cyano doped (—C≡N) symmetric $(m,n=2)$ naphthalene rectifiers. Right: Transmission $T(E)$ for the doped (solid) and undoped (dotted) rectifiers at zero applied bias voltage. The —C≡N substituent shifts the electronic levels near E_F to lower energy, increasing the energy asymmetry and hence decreasing Δ.

$V_{F(R)}$ now correspond to the LUMO crossing either the right or left electrode Fermi levels (see Fig. 7), and the operating voltage range is modified significantly. It is not known if the ''doped'' molecular rectifier of this kind is stable or not (thus, the naphthalene with two CN groups is probably unstable). Nevertheless, the present calculations illustrate the effect of molecular doping, which should be general.

V. CONCLUSIONS

We have presented parameter-free DFT calculations of a class of molecular quantum dots showing current rectification at a reasonable current density through the molecule. The explored mechanism of rectification is different from Aviram-Ratner diodes[1] and relies on a considerable asymmetry of the spatial composition and energy structure of the conducting orbitals of the molecule.[9] Since there are no empirical parameters, the predictions are quantitative and can be tested in a controllable fashion.[11] We have studied molecular quantum dots with a naphthalene central conjugated group, and found a rectification of about 35 for —S—$(CH_2)_2$—$C_{10}H_6$—$(CH_2)_6$—S— molecules. The modest rectification ratio is a consequence of the resonant processes at these molecular sizes. The present design uses relatively short molecules, which, therefore, should not be significantly affected by Coulomb blockade effects, as discussed in the text. The present study also suggests that the rectification ratio in the case of a central single phenyl ring, studied previously,[9] is significantly overestimated by the tight-binding model.

The rectification ratio is not great by any means, but one should bear in mind that this is a device necessarily operating in a ballistic quantum-mechanical regime, because of the small size. This is very different from present Si devices with carriers diffusing through the system. As they become smaller, however, the same effects as those discussed here for molecular rectifiers will eventually take over, and tend to diminish the rectification ratio. In this regard the present results are indicative of the problems which will ultimately be faced by Si devices of molecular proportions.

It is interesting that the parameters of the device, such as the threshold voltages for forward and reverse bias, can be significantly modified by ''chemical'' doping. In the present case adding the −C≡N electron withdrawing group has scaled the threshold range by a factor of about 2. There may be other modifications that could improve/add functionality of the molecular devices, by varying central, end, and side groups of the molecule. The present results illustrate very clearly that the optimization of the parameters of the molecular devices is typically facing the problem that some parameters, such as level widths, vary exponentially, while others, such as the voltage thresholds, vary as a power law as a function of the molecular sizes. Although the approximate band diagrams illustrating the level structure, Fig. 2, are very helpful for a qualitative description, the atomistic details of the electron density distribution are extremely important, Fig. 4. This necessitates the use of *ab initio* methods, without which one may obtain qualitatively wrong results.

We have found that in the present study significant rectification may be obtained in relatively short self-assembled molecules. Self-assembly provides for a good contact with electrodes and relatively small resistance per molecule. In existing studies of Aviram-Ratner-type molecules they were assembled by Langmuir-Blodgett deposition and are prohibitively resistive by design, because of a long aliphatic tail needed for the assembly.[3,4] Thus, for applications the self-assembly of shorter molecules on metallic electrodes seems to be essential. One should keep in mind that the molecular rectification, here estimated for ideal contacts at zero temperature, will be reduced at a finite temperature and also due to inevitable disorder in the contact area and in the molecular film.[25] Indeed, the optimal width of the level was found to be about 12 meV, which is just a half of the room temperature, so the temperature (and static disorder) will significantly broaden the level and reduce the rectification. In terms of the simplest cross-point memories one may use a large number of molecules on a pitch. This may allow for use of longer, better rectifying molecules. There, however, the inelastic processes will play a progressively more significant role[15] and will further reduce the rectification. The present results provide an estimate from above for the rectification ratio of the molecular rectifiers with the present design. Further studies of molecular rectifiers should be focused on these outstanding issues in conjunction with experimental studies.

ACKNOWLEDGMENTS

We acknowledge useful discussions with Shun-chi Chang and R. S. Williams. The work was supported by DARPA.

[1] A. Aviram and M.A. Ratner, Chem. Phys. Lett. **29**, 277 (1974).
[2] J.C. Ellenbogen and J.C. Love, Proc. IEEE **88**, 386 (2000).
[3] A.S. Martin, J.R. Sambles, and G.J. Ashwell, Phys. Rev. Lett. **70**, 218 (1993).
[4] R.M. Metzger, B. Chen, U. Höpfner, M.V. Lakshmikantham, D. Vuillaume, T. Kawai, X. Wu, H. Tachibana, T.V. Hughes, H. Sakurai, J.W. Baldwin, C. Hosch, M.P. Cava, L. Brehmer, and G.J. Ashwell, J. Am. Chem. Soc. **119**, 10 455 (1997).
[5] C. Krzeminski, C. Delerue, G. Allan, D. Vuillaume, and R.M. Metzger, Phys. Rev. B **64**, 085405 (2001).
[6] C. Zhou, M.R. Deshpande, M.A. Reed, L. Jones II, and J.M. Tour, Appl. Phys. Lett. **71**, 611 (1997).
[7] Y. Xue, S. Datta, S. Hong, R. Reifenberger, J.I. Henderson, and C.P. Kubiak, Phys. Rev. B **59**, 7852 (1999).
[8] J. Reichert, R. Ochs, D. Beckmann, H.B. Weber, M. Mayor, and H.v. Löhneysen, Phys. Rev. Lett. **88**, 176804 (2002).
[9] P.E. Kornilovitch, A.M. Bratkovsky, and R.S. Williams, Phys. Rev. B **66**, 165436 (2002).
[10] S. Lenfant, C. Krzeminski, C. Delerue, G. Allan, and D. Vuillaume, Nano Lett. **3**, 741 (2003).
[11] S. Chang, Z. Li, C.N. Lau, B. Larade, and R.S. Williams, Appl. Phys. Lett. **83**, 3198 (2003).
[12] J. Taylor, H. Guo and J. Wang, Phys. Rev. B **63**, 121104(R) (2001); **63**, 245407 (2001).
[13] A.S. Alexandrov and A.M. Bratkovsky, Phys. Rev. B **67**, 235312 (2003).
[14] N.B. Zhitenev, H. Meng, and Z. Bao, Phys. Rev. Lett. **88**, 226801 (2002).
[15] C. Boulas, J.V. Davidovits, F. Rondelez, and D. Vuillaume, Phys. Rev. Lett. **76**, 4797 (1996).
[16] Molecular coordinates are initially relaxed using the GAUSSIAN98 program (Ref. 17), in the absence of the Au electrodes. No further relaxation occurs and transport calculations proceed assuming a static conformation of the electrode-molecule-electrode system.
[17] M.J. Frisch *et al.*, GAUSSIAN98, Revision A.9 (Gaussian Inc., Pittsburgh, PA, 1998).
[18] A.P. Jauho, N.S. Wingreen, and Y. Meir, Phys. Rev. B **50**, 5528 (1994); S. Datta, *Electronic Transport in Mesoscopic Systems* (Cambridge University Press, New York, 1999).
[19] S. Sanvito, C.J. Lambert, J.H. Jefferson, and A.M. Bratkovsky, Phys. Rev. B **59**, 11 936 (1999).
[20] N. Troullier and J.L. Martins, Phys. Rev. B **43**, 1993 (1991).
[21] O.F. Sankey and D.J. Niklewski, Phys. Rev. B **40**, 3979 (1989).
[22] P. Ordejon, E. Artacho, and J.M. Soler, Phys. Rev. B **53**, R10 441 (1996)
[23] In our calculations, the ''molecule'' HOMO and LUMO states for an open system are determined by extracting the molecular subset of our self-consistent Hamiltonian matrix and diagonalizing this to obtain the ''interacting'' molecule energy levels, accounting for the presence of atomic electrodes and any externally applied bias or gate potentials, see Ref. 24.
[24] B. Larade, J. Taylor, Q.R. Zheng, H. Mehrez, P. Pomorski, and H. Guo, Phys. Rev. B **64**, 195402 (2001).
[25] A.M. Bratkovsky and P.E. Kornilovitch, Phys. Rev. B **67**, 115307 (2003).